

# MULTIPOLE AND ALIGNMENT ERROR LIMITS FOR THE SESAME STORAGE RING MAGNETS

M. Attal, E. Huttel, SESAME, P.O. Box 7, Allan 19252, Jordan

## Abstract

SESAME storage ring magnets are being constructed through the CESSAMag project in the frame of SESAME - CERN/EU collaboration. The impact of multipole and alignment errors in these magnets on machine performance have been investigated using different tracking codes. The lattice tolerances for both systematic and random errors are defined. This article reports on the investigation results.

## INTRODUCTION

A large dynamic aperture is required for a reasonable beam lifetime and high injection efficiency in a 3<sup>rd</sup> generation light source. In SESAME the criteria is that the dynamic aperture size should keep exceeding the machine physical acceptance when machine errors are taken into account mainly high order multipoles which are a main source of dynamic aperture destruction.

Since SESAME storage ring magnets started to be constructed, through CESSAMag project [1] provided by CERN / EU collaboration, defining the detailed machine tolerance for such magnetic errors is a requirement. The high order multipole terms used are obtained from the magnetic flux expansion [2]:

$$B_y + iB_x = \sum_{n=1}^{\infty} (b_n + ia_n)(x + iy)^{n-1} \quad (1)$$

where  $b_n$ ,  $a_n$  are coefficients of the normal and skew  $2n$ -pole components respectively. The corresponding relative magnetic errors at mid plane are given by  $B_n / B_N$ ,  $A_n / B_N$  where  $B_n = b_n x^{n-1}$ ,  $A_n = a_n x^{n-1}$  with  $N = 1, 2, 3$  for dipole, quadrupole and sextupole.

## TRACKING PARAMETERS

SESAME lattice is a Double-Bend Achromat with dispersive straight sections as shown in Fig. 1. The design working point is (7.23, 6.19) and emittance is 26 nm.rad. Two tracking codes, for crosscheck, BETA [3] and Accelerator Toolbox [4] are used to evaluate the multipole effect on SESAME dynamics. To understand the internal resonance structure of dynamic aperture, the Frequency Map Analysis (FMA) technique [5] is used with particle tracking done using TRACY-2 code [6].

The dynamic aperture calculations are carried out, for both chromaticities = +5, at middle of the long section which has an acceptance aperture of  $x = \pm 23$  mm,  $y = \pm 3.5$  mm as defined by vacuum chamber and injection

septum limitations, scaled to the optical functions. For the final results the particle is tracked for 5000 turns.

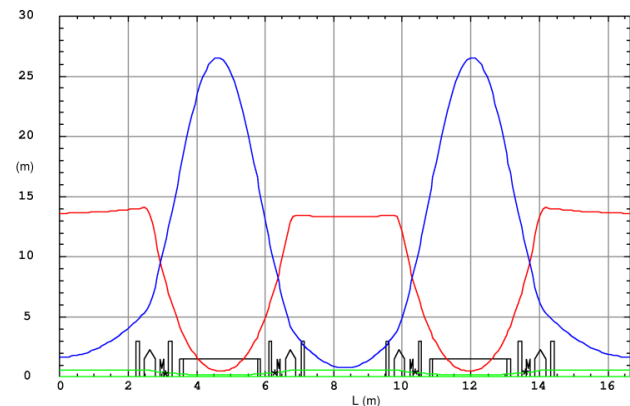


Figure 1: SESAME storage ring optics showing  $\beta_x$  (red),  $\beta_z$  (blue) and dispersion  $\eta_x$  (green).

## MAGNETIC ERROR TOLERANCES

In this investigation the lattice tolerance for each multipole component is defined individually first, to see how destructive each one is. Then, all multipole contents in all magnets are combined together. If the total effect becomes out of the lattice tolerance, strengths of the components are reduced one by one starting with the most destructive ones. Table 1 shows the lattice tolerance for the main high order multipoles, *systematic* and *random*, calculated at  $x = 20$  mm in dipole and  $x = 24$  mm in quadrupole and sextupole. Sextupole contents include also the ones created by the orbit and coupling correcting coils. Figure 2 shows the on-momentum dynamic aperture, tracked for 5000 turns, under two extreme cases of multipole effect when all components have the same sign. It can be seen that the final size of dynamic aperture is still larger than the machine physical acceptance. The sextupole high order component is not critical and the corresponding chromaticity variation can be easily compensated with the strength-relaxed sextupoles.

### Deeper Analysis Using Frequency Map

For a deep insight into the mechanism in which dynamic aperture is destroyed, the Frequency Map Analysis is used. Figure 3 shows the high order multipole effect on on-momentum dynamic aperture when all components have positive signs. The dynamic aperture structure shows different levels of particle stability ranging from the very stable particle (blue) till the chaotic one (red). The corresponding tune shift and destruction driving resonances are displayed by the frequency map in Fig. 3(bottom) and listed in Table 2 where systematic

resonance means the one that drives the working point to an integer a multiple of the storage ring symmetry.

Table 1: Tolerable  $B_n/B_N$ ,  $A_n/B_N$  in SESAME Magnets

Multipole component	Dipole N = 1	Quadrupole N = 2	Sextupole N = 3
$B_4/B_N$	$\pm 1 \times 10^{-3}$	$\pm 1 \times 10^{-3}$	$\pm 1 \times 10^{-1}$
$B_5/B_N$	$\pm 1 \times 10^{-3}$	$\pm 1 \times 10^{-3}$	$\pm 1 \times 10^{-1}$
$B_6/B_N$	$\pm 6 \times 10^{-4}$	$\pm 6 \times 10^{-4}$	
$B_7/B_N$	$\pm 1 \times 10^{-3}$		
$B_9/B_N$			$\pm 2 \times 10^{-3}$
$B_{10}/B_N$		$\pm 1 \times 10^{-3}$	
$B_{14}/B_N$		$\pm 2 \times 10^{-4}$	
$B_{15}/B_N$			$\pm 1 \times 10^{-3}$
$A_3/B_N$		$\pm 2 \times 10^{-3}$	
$A_4/B_N$		$\pm 2 \times 10^{-3}$	
$A_5/B_N$		$\pm 1 \times 10^{-2}$	$\pm 1 \times 10^{-1}$

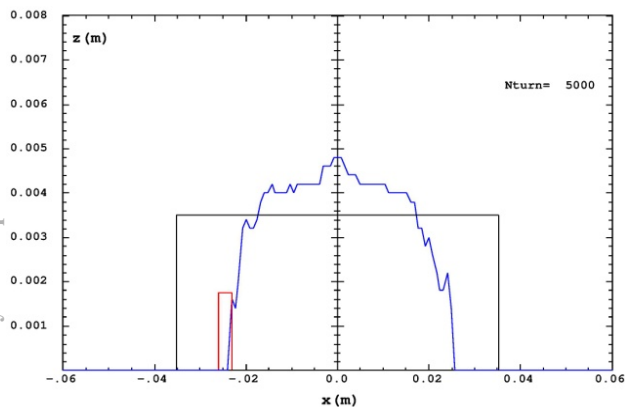
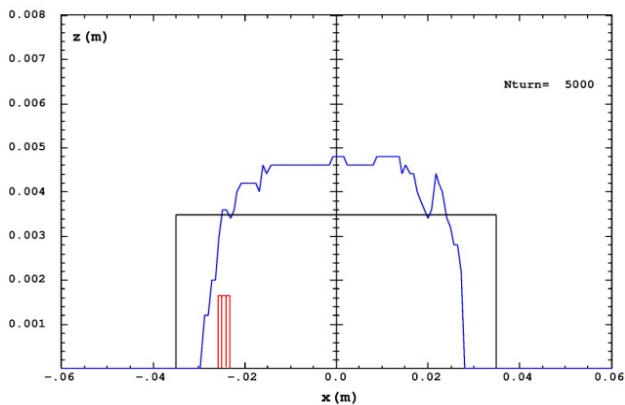


Figure 2: Dynamic aperture under high order multipole effect, with positive sign (top) and negative sign (bottom) for all components. The black rectangle represents acceptance of vacuum chamber, whereas red bars represent injection septum sheet limitation.

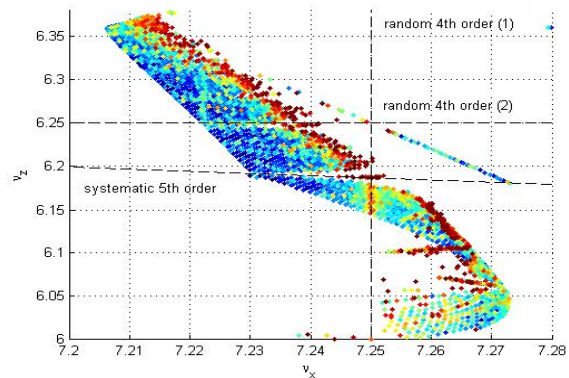
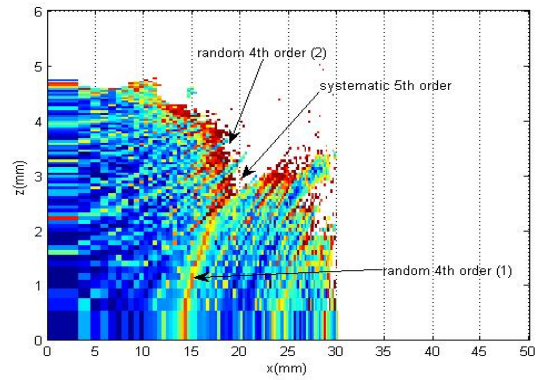


Figure 3: Dynamic aperture of on-momentum particle (top) and the corresponding frequency map (bottom).

Table 2: Most Effective Resonances

Resonance	Resonance equation
Systematic 5 <sup>th</sup> order	$Q_x + 4Q_z = 32$
Random 4 <sup>th</sup> order (1), (2)	$4Q_x = 29, 4Q_z = 25$

The general shrink noticed in dynamic aperture is due to the common effect of high order multipoles. However the analysis show that the most critical ones are the octupole, and decapole components which penetrate the dynamic aperture deeply creating regions of nonlinear particle motion then chaotic ones at higher amplitude through exciting random 4th order and systematic 5th order resonances. The decapole component is a systematic one created by the dipole pole geometry. On the other hand it can be a random as well as the octupole component which are created due to construction errors in dipole and quadrupole magnets. Figure 3 shows that these components can severely minimize the dynamic aperture if the magnets are not carefully constructed.

Figure 4 displays dynamic apertures and frequency maps of  $\pm 1.5\%$  off-momentum particles which clearly see different types of resonances however keep stable up to reasonable transverse amplitudes.

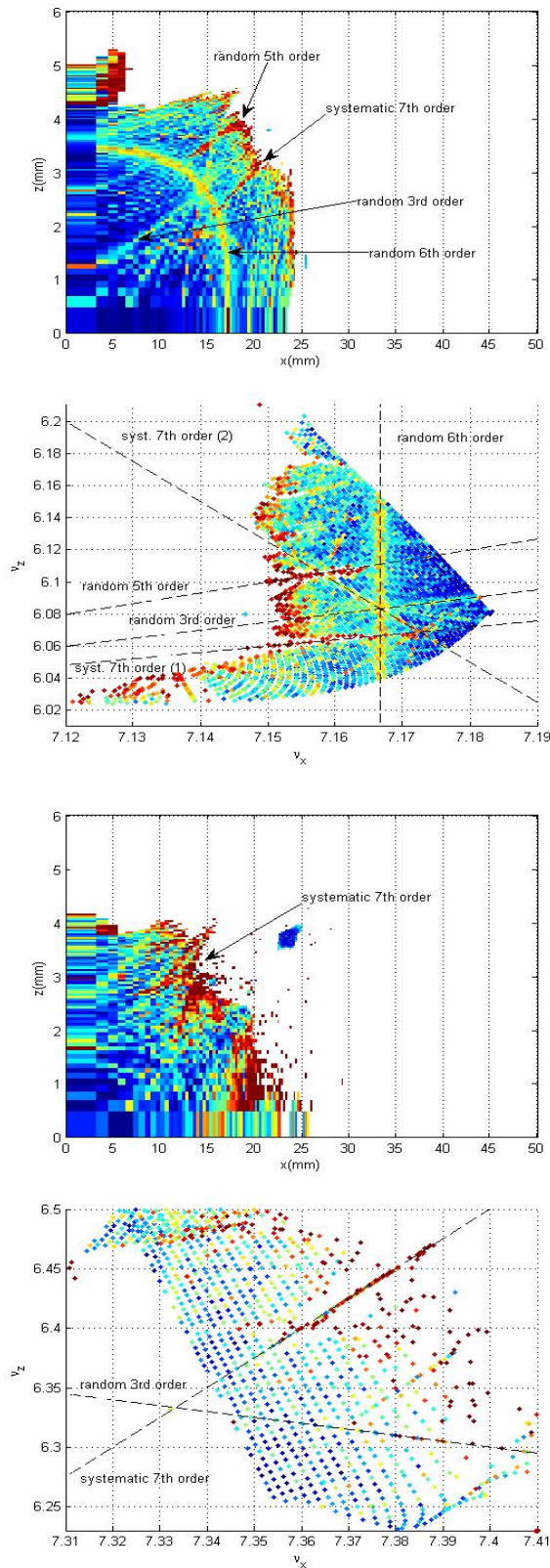


Figure 4: Dynamic apertures and corresponding frequency maps of -1.5% (top, second) and 1.5% (third, bottom) off-momentum particles.

It is worth mentioning that effect of 5th order resonance can be mitigated by changing the fractional tunes [7].

### MAGNET MISALIGNMENT TOLERANCES

SESAME optics is sensitive to the vertical magnetic misalignment due to the high vertical beta function  $\beta_z$  in mid of the bending magnet. The criteria used to define the misalignment tolerances are the amplitude of closed orbit distortion before correction which should be less than 4 mm rms [8], the corrector power needed for correction, and the residual orbit and optical distortions. The 1rms misalignment tolerances are listed in Table 3. The 0.5 mm tolerances are based on reasonable mechanical tolerances. The error distribution should be cut at  $2\sigma$ .

Table 3: Magnet Misalignment Tolerances

Magnet misalignment	Tolerance value (1rms)
Dipole dx, ds	0.5 mm
Dipole dy, $d\phi_s$	0.1 mm, 0.2 mrad
Dipole $d\phi_x, d\phi_y$	0.5 mrad
Quadrupole dx, dy	0.1 mm
Sextupole dx, dy	0.2 mm
Quadrupole/ Sextupole ds	0.5 mm
Quadrup./ Sext. $d\phi_x, d\phi_y$	0.2 mrad

### CONCLUSION

SESAME lattice has relaxed tolerances on magnetic errors due to the not strong focusing compared to the modern 3<sup>rd</sup> generation light sources. However the vertical magnet misalignment is more restricted in case of the combined-function bending magnet but, nevertheless, still within the achievable alignment tolerance.

### REFERENCES

- [1] A. Milanese, E. Huttler, M. Shehab, IPAC14, these proceedings.
- [2] J. Rossbach, P. Schmuser, “Basic Course on Accelerator Optics”, CERN Acc. Sch., CERN 94-01.
- [3] BETA, J. Payet. CEA/DSM/ Irfu/ SACM, <ftp://ftp.cea.fr/incoming/y2k01/beta/>
- [4] A. Terebilo, SLAC-PUB-8732.
- [5] H. S. Dumas, J. Laskar, Phys. Rev. Lett. 70, 2975-2979 (1993).
- [6] J. Bengtsson, E. Forest and H. Nishimura, ‘Tracy User Manual’, unpublished (ALS, Berkeley).
- [7] M. Attal, Proceedings of IPAC13.
- [8] M. Attal, Tech. Note, SES-TE-AP-TN0001.